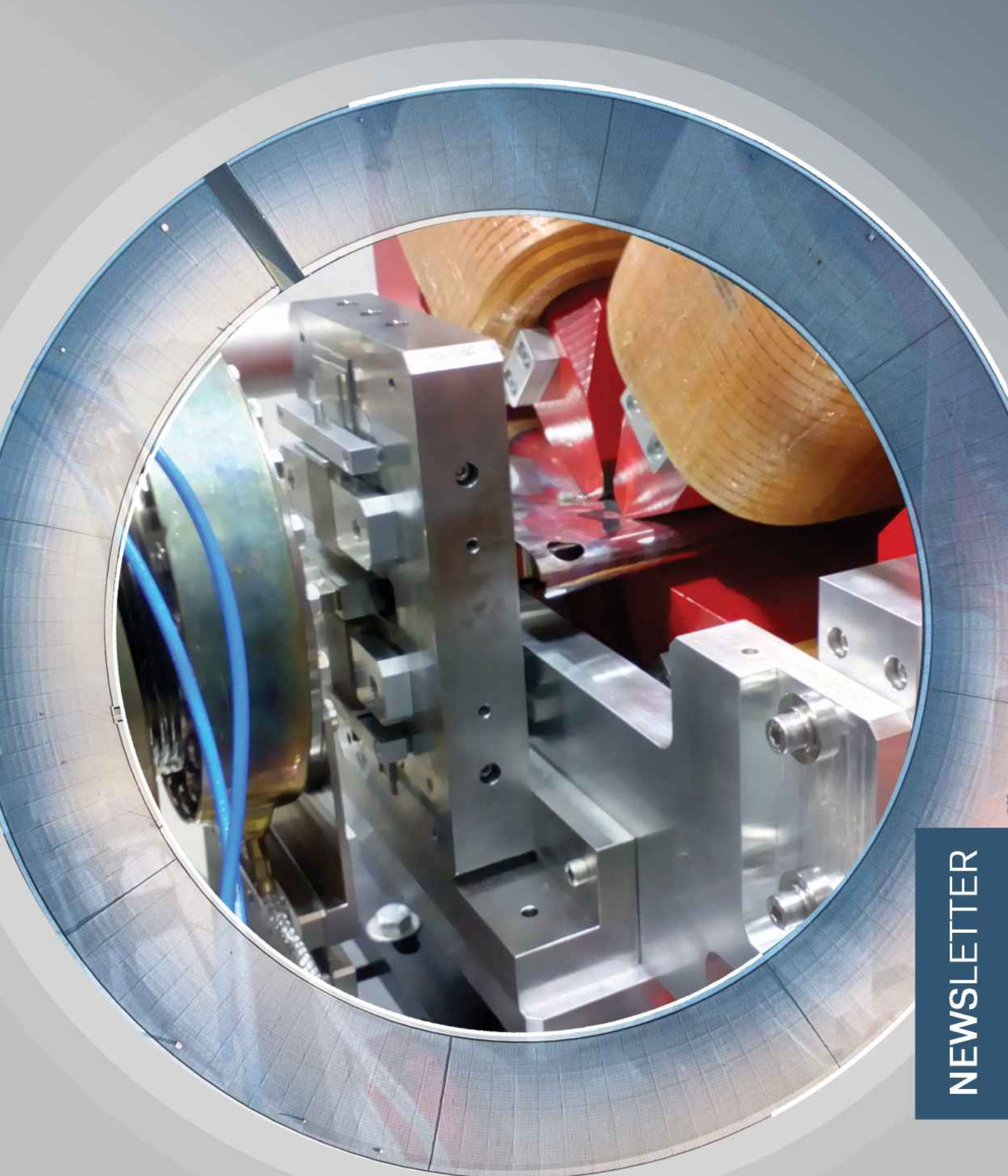


2019

XMaS



NEWSLETTER

- 2 | Directors' Corner
- 3 | Public Outreach
- 4 | XMaS Upgrade
- 6 | Materials Science
- 8 | Condensed Matter
- 9 | Healthcare
- 10 | Soft Matter
- 12 | Energy & Catalysis
- 14 | Access to Synchrotron and Offline Facilities
- 15 | Beamline people

Directors' Corner

As we are sure you are all aware the ESRF has been down since December 2018. The old machine was dismantled in less than three months with our long serving BM28 dipole disassembled and entirely recycled. The upgrade to the Extremely Brilliant Source (EBS) is, at the time of writing, on-track with machine commissioning underway. Electrons should soon be regularly circulating around the ring with planned interventions to install and commission the short-bend sources. Once we have beam, we will need a couple of months to commission the beamline so as to be ready to accept users at the end of August. Note that there are likely to be some start up gremlins so we thank our new first users in advance for their understanding. Fingers crossed for a smooth and on-time commissioning period. We expect the next call for user proposals to be March (ESRF) and April (XMaS) 2020. In addition, we have reserved time for rapid access for industrial work. Please get in touch if we can help for either proprietary studies or feasibility case-studies.

As a result of all the necessary upgrade preparations, 2019 has been a completely different year for the facility with very little scientific research and a whole lot of redesigning, rebuilding and engineering. We are indebted to EPSRC for providing the funds to facilitate a refurbishment

of the beamline's core components. Given that most of these have seen more than 20 years of service, the upgrade is a welcome opportunity to refurbish and replace many of the key components. The centrepiece instrument, the diffractometer, is being reconditioned by Huber and will come back as good as new with a strengthened detector arm with two scattering pathways, one for point detectors and the other for the suite of 2D detectors.

After much discussion, both in house and with our users, we rejected the "simple solution" of making our updated beamline solely a focussed monochromatic beam facility, despite the fact that the majority of our experiments take place in that mode. We have engineered the "new" beamline like the old one to permit the use of an unfocussed monochromatic beam, which will be of interest to those for whom a lower power density is important. We have also preserved the potential for white beam studies, although this will require further work and safety upgrades when we get back in business. Further details are given in the section describing the beamline upgrade (pages 4-5). By the time this Newsletter is out, the new equipment will be being put together and aligned. Regular updates will continue to be given on our twitter feed (@XMaSBeam #XMaUpgrade).

All this activity has represented a heavy workload for all the XMaS staff during 2019 with complex project planning and management needed to bring it all together. Despite this focus on rebuilding activities, we have attempted to maintain our interaction with users. The annual XMaS User meeting was held at the University of Warwick in November 2019 with over 50 attendees. The hugely successful "*X-ray & Neutron Scattering in Multiferroics Research*" series was continued into its 5th meeting. Held at the IOM3 in February 2019, the meeting was co-organised by XMaS, Electrosciences and the Smart Materials & Systems Committee of the UK's Institute of Materials, Minerals and Mining. We welcomed several prominent international speakers and this vibrant event was enjoyed by all.

Happily, some science has still been performed on the beamline, with the offline facility used extensively over the past year. Although the beamline has not been operational, user publications have not slowed down and have continued the trend of increasing scientific output being found in high impact journals. Please read on for some highlights from the past year. It is gratifying to record that user appreciation of the beamline and the support staff is very high.

The *XMaS Scientist Experience* competition [1] allowed a 16-strong group of enthusiastic female A-level students to visit the ESRF, talk to female scientists about their diverse career paths and take part in the ESRF's Synchrotron@School programme [2]. The only thing they could not do was to visit the actual XMaS beamline which was in pieces due to our upgrade work. The sixth competition is now launched, and we anticipate an ever widening participation from students across the UK.

If you would like to receive XMaS updates including beamtime application reminders by email and are not currently included in our mailing-list, please visit [3].

Finally, looking forward, we will be augmenting the onsite team with the appointment of two post-doctoral researchers who will support users and further develop metrology tools for the wider community. Please keep an eye out for the advertisements in early 2020.

Malcolm Cooper, Yvonne Gründer, Tom Hase and Chris Lucas

Empowering young women to pursue careers in STEM

The *XMaS Scientist Experience* is a nationwide competition [1] aimed at encouraging young women to consider careers in science, by showing them some opportunities available to them and introducing them to inspirational role models, all within the international setting of the EPN campus [2]. The applicants are required to write about a famous female scientist, her contribution to promoting the cause of women in science and their own motivation for entering the competition. The prize for the competition winners is a 5 day trip to Grenoble, France. The group of up to 16 year-12 female students visits the ESRF, including XMaS, as well as nearby laboratories. A major part of the trip is to take part in the Synchrotron@School programme run by the ESRF. The winners also share a lunch with women scientists, engineers, technicians and students who work there: there is one woman available for every 2 girls, which allows for in-depth conversations. These meetings carry on after lunch over coffee. After the trip, the girls share their experiences with family and friends and their peers, further

influencing the views of the students' support groups.

Both winners and their families have been full of praise for the initiative. The *XMaS Scientist Experience* has allowed its winners to experience what life as a scientist could be, far from the clichés that still exist. As female students, many stressed how empowered they felt after the trip. Charlotte declared: *"This whole experience has been absolutely incredible – it has shown me the whole world of opportunities there are out there for women in science, and that a career in physics isn't out of my reach"*. All the winners we have managed to follow over the years went on to study STEM (Science, Technology Engineering Mathematics and Medicine) at university, with two currently studying Physics at the University of Warwick.

Winners are keen to act as ambassadors and advertise the competition amongst their peers, often with winners writing a piece in their schools' newsletters. The

programme is also receiving a lot of attention on social media (@XMaSSchoolTrip, @XMaSBeam) as well as recently in more mainstream media, including STEMettes Monday Motivation and BBC Radio Coventry and Warwickshire as part of the Vic Minnett Show (Fig. 1). The winners are also an integral part of the annual Warwick Science Gala, which is an evening for school pupils of all ages promoting STEM in an interactive environment.

The *XMaS Scientist Experience* has now been running for 5 years, allowing us to reflect on the outcomes of the trips. The enthusiasm of the participants afterwards is remarkably positive and they all comment that it is an eye-opener to the roles that they could play as future women in science. The first few years' entrants came only from schools located near the XMaS hubs of Liverpool and Coventry (Warwick) areas. Applicants come now from schools located as far away as Kent and Essex. We have now actively started to target students from Widening Participation backgrounds, devoting specific spaces on the 2020 trip to females from such backgrounds.

We would be happy to collaborate with XMaS users interested in publicising the competition in their local area, as we are looking to create more nodes to expand our network. Please do not hesitate to get in touch!

[1] www.xmas.ac.uk/impact/xmas_scientist_experience

[2] www.epn-campus.eu

Fig. 1: Vic Minnett Show, 19th July 2019. Left to right: Elizabeth Clennell (2019 winner), Ally Caldecote (University of Warwick, Physics Department), Charlotte Jackson (2017 winner).



For more information contact:
N. Borrel, Department of Physics,
University of Warwick, Coventry, UK.
N.Borrel@warwick.ac.uk

A new beamline!

Since the last edition of the XMaS Newsletter, the ESRF machine has entered a new era with December 6th 2019 a key milestone as electrons were stored for the first time in the new EBS storage ring. The machine team has been working hard ever since to reach the beam parameters required to restart the experimental programme by March 2020. Once the new machine has been tamed/mastered, the next step is to open the Insertion Device (ID) beamline front ends (January). The Bending Magnet (BM) beamlines (13 CRGs and 4 ESRF beamlines), which were seriously impacted by the new lattice, come next with the installation of the first 'short-bend' (SB) and '2-pole wiggler' (2PW) during the February shutdown. The machine parameters will require further adjustment after the insertion of those SB and 2PW magnets. The remaining SBs, 2PWs and 3PWs will be installed between March and April. The commissioning of the beamline will resume at the end of July, with planned user operations beginning at the end of August 2020.

Meanwhile, the beamline itself has been transformed many times over the last ten months with all the cabins alternatively looking more like storage spaces rather than a real beamline depending on where the heavy work was taking place. Regular updates have appeared on social media (@XMaSBeam, #XMaSupgrade). More recently, the cabins have started to look more like a new beamline being built! New floors, equipment moved to their new positions, etc...

Optics Hutch

The new position of our EBS short-bend source necessitated major modifications to the whole beamline starting from the first element in the optics hutch (OH1). The front end port coming from the machine was displaced laterally towards the ring by ~10 cm. OH1 was completely realigned [1] to accommodate the

new x-ray beam path and characteristics (wider energy spectrum, higher heat load, smaller beam). We re-used as much of the old equipment (slits vessels, beryllium windows, safety shutter, stands,...) as possible. The cryogenically cooled monochromator [1], installed in September 2018, was craned into its new position and the new toroidal mirror system [2] (Fig. 2) is almost ready to be installed. The new beamline optics will offer a working energy between 2.035 and 41 keV, with the mirror energy cut-off at 33 keV.

An additional two pieces of equipment are being installed into the optics hutch. A water cooled white beam attenuator/monitor [3] will allow the insertion of pyrolytic graphite sheets into the beam, reducing the heat load on the monochromator during high energy experiments (above 20-30 keV). The system is also equipped with a detector to view the x-ray beam. A water cooled Densimet® block (white beam stop) will be mounted upstream of the focusing mirror to prevent the white beam from entering the experimental hutch (EH1), which is no longer white beam compatible. We hope that white beam operation may still be possible in EH1 in a near future but with a reduced beam size.

Middle Cabin

Major modifications were applied to the cabin located between OH1 and



Fig. 2: The new toroidal mirrors system during the factory acceptance tests at IRELEC [2] in January 2020.

EH1. The room has been enlarged after the removal of an unused ventilation system. The XMaS team handled the tricky task of moving the 15m long lead-shielded stainless steel tubes towards the ring to align them to the new beam path. A new floor has also been installed. This refreshed cabin will offer a larger and friendlier workspace with new laboratory equipment such as a hydraulic powder press, a Nikon stereomicroscope and a micro balance. The fume hood will remain for the handling of small volumes of volatile liquids and hazardous materials such as powders. As before, where more stringent containment

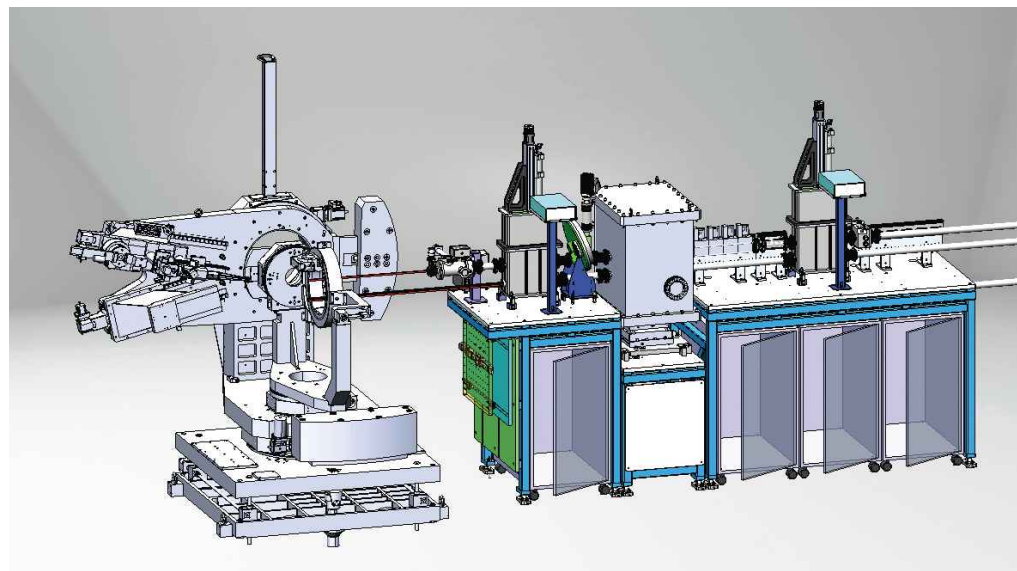


Fig. 3: 3D view of the new beam delivery of the experimental hutch.

requirements are needed, these experiments must be performed in the ESRF/ILL Chemical Laboratory.

Experimental Hutch

After the EH1 hutch extension in May 2018, a new beam delivery system (Fig. 3) was conceived to accommodate the new beam characteristics whilst retaining the three beam operational modes previously available on the beamline, i.e. the monochromatic focused beam (MFB), the monochromatic unfocused beam (MUB) and the white beam (WB) mode. The EH1 entry slits vessel was redesigned [1] to accommodate the new MFB position, but re-employing the actual slits, ion pump and gauges. The harmonic rejection mirrors (HRM) will be upgraded, replacing the old Pyrex® mirrors with two new silicon substrates, each of them having three stripes (Rh and Pt coatings together with bare Si) in order to cover the wider energy spectrum of the upgraded beamline. Both the HRM mechanics and vacuum chamber will be re-used, with the latter being slightly modified to keep the WB and MUB capabilities.

A new incident beam intensity monitoring system is being designed [3]. This new system consists of two retractable in-vacuum ion chambers (ICs) and variable thickness scatter foils to enable efficient operation over the 2-41 keV energy range. An IC monitor system is probably

more beneficial above 4 keV, whilst a simple scatter foil can produce a good monitor signal without significantly degrading the transmitted flux at low energies. The in-vacuum IC units can be driven independently to the different beam positions, or removed entirely allowing a windowless vacuum path for the incident beam at low energies. The scatter foil monitor system also allows for a range of different reference foils to be placed into the beam, allowing quick and easy energy calibrations. The two in-vacuum ICs are placed



either side of these reference foils. A new gas handling/mixing system is being designed to deliver a range of gases to these ICs and the sample environment (Fig. 4).

More attenuator banks were purchased to cover the extended energy spectrum. Phase-plate crystals (diamond and Si) used as polarisation conditioners between 2.4 and 14 keV, will be permanently mounted and kept under vacuum in a new dedicated system [4]. The beam delivery will be terminated by a vacuum vessel [3] comprising both a fast shutter and a beam position monitor system (XBPM). The XBPM is based on a quad-diode concept [5] that can be used in fluorescence mode (backscattering) to increase efficiency. It can also monitor the polarisation of the beam after the phase plate, using quad-diodes in forward scattering.

Finally the diffractometer is being refurbished and upgraded [4] to have a double 2θ arm, one for

mounting 2D detectors and one for the (conventional or polarisation) analysers and slits. The refurbished diffractometer will sit 3 m downstream and ~25 cm sideways from its old position. New 2D detectors (Lambda 750 CdTe from X-Spectrum and a Pilatus3-S-1M from Dectris) have been purchased to complete the suite of existing detectors. The GI-SAXS rail is being modified [6] to take into account the extra space derived from the hutch extension and the new diffractometer position.

Fig. 4: New gas handling system to keep all the gas bottles for sample environment and ionisation chambers outside the experimental hutch.

Finally, all the beamline motor drivers have been upgraded to IcePAPs. The electrical noise level will be reduced by reducing the length of cables (motors, signal, power), an asset when measuring low level signals. The beamline will restart with our current SPEC control before a migration to the new ESRF control software BLISS only when it has been fully tested.

[1] ERIA (www.eria.gandi.ws)

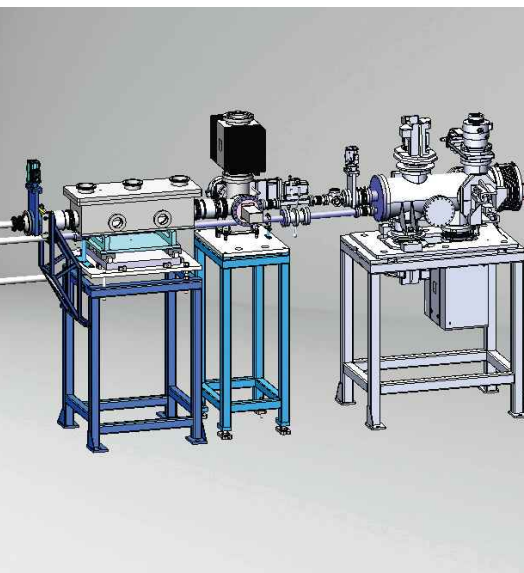
[2] IRELEC (www.irelec-alcen.com)

[3] Design et Mécanique (harris@design-mecanique.fr)

[4] Huber Diffractionstechnik GmbH (www.xhuber.de)

[5] R.W. Alkire, J. Synchrotron Rad. 7, 61 (2000); S.R. Marques, Proc. of EPAC08, TUPC064, 1200 (2008); S. Collins, AIP Conf. Proc. 1234, 303 (2010).

[6] Nominal Ingénierie (www.nominal-ingenierie.business.site)



Perovskite-polymer bulk heterostructures for efficient LEDs

B. Zhao, M. Alsari, S. Lilliu, R. H. Friend, D. Di *et al.*

Since the demonstration of bright perovskite based light emitting diodes (LEDs) in 2012 by Tan *et al.* [1], tremendous attention has been focused on improving the LED efficiency and understanding the underlying mechanisms. The external electroluminescence efficiency, for example, improved from ~1% to 12% [2,3] before 2018.

In this work [3], we demonstrate perovskite-polymer (poly-HEMA*) bulk heterostructures (PPBH) with photoluminescence quantum efficiencies (PLQE) of up to 96%. Importantly, we achieved a record-breaking external electroluminescence quantum efficiency (EQE) of more than 20% in LEDs based on our perovskite-polymer materials through the complete elimination of non-radiative decay processes. The emissive heterostructures are prepared from a combination of quasi-2D/3D perovskites and a wide optical gap polymer, poly-HEMA. Grazing Incidence Wide Angle X-Ray Scattering (GI-WAXS) measurements indicate that the perovskite

crystallites are isotropically oriented within the PPBH film (Fig. 5a). High-resolution transmission electron microscopy (HR-TEM) results suggest the presence of quasi-2D and 3D crystal structures (Fig. 5b).

To investigate the electroluminescence (EL) properties of the PPBH, we developed a solution-processed multilayer LED structure. The peak EQE of the best devices reaches 20.1% (Fig. 5c), representing a record for perovskite-based LEDs. The efficiencies of our perovskite-based LEDs are on a par with those of the best OLEDs [4-6] and quantum-dot (QD) LEDs [7].

In addition, we carried out a thorough investigation of the light emission process, using ultrafast spectroscopy. The spectroscopic results reveal that upon excitation, photogenerated excitons at the quasi-2D perovskite component migrate rapidly to low-energy sites within 1 ps. Transient Absorption (TA) experiments (Fig. 5d) confirm that the initial photoexcitation is formed on the quasi-2D perovskite, with a

ground-state bleach (GSB) peak at ~575 nm. The GSB feature related to the bi-layer quasi-2D perovskite has an exciton-like character, suggesting the electron-hole pair created in the material is initially bound. As the 575 nm GSB quickly decays, a red-shifting, broad GSB signal rises rapidly and then declines after 10 ps. Coupled with the high PLQE and negligible luminescence quenching at the interfaces, we found non-radiative pathways to be effectively eliminated.

Furthermore, conventional optical models indicate that the high EQEs achieved benefit from the reduced effective refractive index, which improves the optical coupling. The 20% EQE is further supported by ~100% internal EL efficiency from our modelling. The rapid energy migration, the effective suppression of non-radiative events and the reduced effective refractive index lead to the high efficiency of perovskite-polymer bulk heterostructure LEDs.

* poly(2-hydroxyethyl methacrylate)

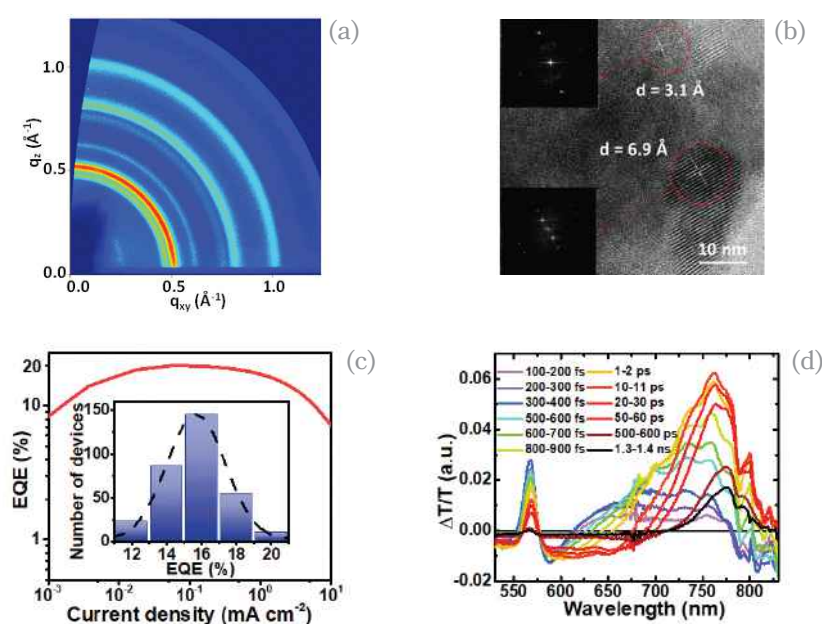


Fig. 5: (a) GI-WAXS patterns of a PPBH film. (b) HR-TEM image of a PPBH film. Insets show the fast Fourier transforms of the crystalline regions, exhibiting quasi-2D and 3D structures. (c) EQE-current density characteristics of the best PPBH LED and peak EQE statistics (inset). (d) TA spectra of the sample.

- [1] Z.-K. Tan *et al.*, Nat. Nanotechnol. 9, 687 (2014).
 [2] N. Wang *et al.*, Nat. Photon. 10, 699 (2016).
 [3] B. Zhao *et al.*, Nat. Photon. 12, 783 (2018).
 [4] S. Reineke *et al.*, Nature 459, 234 (2009).
 [5] H. Uoyama *et al.*, Nature 492, 234 (2012).
 [6] D. Di *et al.*, Science 356, 159 (2017).
 [7] X. Dai *et al.*, Nature 515, 96 (2014).

For more information contact:
 B. Zhao, Cavendish Laboratory,
 University of Cambridge, UK.

bz246@cam.ac.uk

Assessing the solubility of spent nuclear fuel

S. Yadukrishnan, W.J. Nuttall, R. Springell

Spent Nuclear Fuel (SNF) or the fuel retrieved after its useful lifetime in a nuclear reactor is thermally hot. It is therefore stored in cooling ponds before being transferred into dry casks for intermediate or long-term storage where it continues radioactive decay for tens of thousands of years. In the event of a premature barrier failure, there is a possibility that groundwater or fuel pond water can come into direct contact with highly active spent fuel.

Nuclear fuel, which is predominantly UO_2 , is insoluble in water in its stable state; however, the radioactive environment means that this fuel-water system quickly becomes vulnerable to a complicated redox reaction as water radiolyses into a number of ions, radicals and combined molecular products (such as H_2O_2 & H_2). These radiolysis products may have different effects depending on the interacting surface atom of the spent fuel matrix. For example, UO_2 , under oxidising conditions, can form UO_2^{2+} (uranyl) which is readily soluble, risking an accelerated dissolution of the fuel matrix. Therefore, understanding the behaviour of radioactive SNF in the presence of water is vital in predicting short and long-term effects in the unlikely event of a cladding failure.

Through previous experiments, we have successfully investigated the corrosion phenomena studying idealised SNF samples [1]. Using a technique involving synchrotron x-rays to produce a local radiolytic environment over epitaxial thin film samples, we have been able to assess the rate of corrosion in UO_2 and CeO_2 (a non-radioactive surrogate for PuO_2) using a combination of x-ray reflectivity and high-angle diffraction. The dissolution phenomenon gets more complicated in the case of real SNF

as it is also affected by the presence of other constituents such as fission product inclusions and transuranics. For example, the dissolution rates of uranium and plutonium depend on the ease of oxidation, or reduction, of the surface atoms (in a radiolytic atmosphere) as their individual solubilities depend on their oxidation states [2]. This led us to explore the (U, Ce) O_2 mixed oxide (MOX) films as a proxy for (U, Pu) O_2 systems as these allow for more realistic SNF corrosion scenarios to be studied. We selected hydrogen peroxide to simulate the radiolytic end products of water and exposed our pristine MOX samples (of various U to Ce concentrations) to a 0.1M solution of H_2O_2 . The concentration was selected to reproduce the radiolytic environments seen in our synchrotron experiments [1]. The film was exposed for different timescales in order to measure the rate of oxidative corrosion as a function of exposure time. The corrosion was recently probed using a combination of X-Ray Reflectivity (XRR) and high angle diffraction at the **offline laboratory source** at XMaS.

Contrary to the high solubility seen in our UO_2 experiments, the MOX films showed no measurable corrosion despite the uranium content in the matrix (Fig. 6). This opens up interesting questions regarding the precise mechanisms of SNF dissolution and the results presented here highlight the need to understand the role of individual SNF species in this mechanism.

[1] R. Springell *et al.*, Faraday Discuss., 180, 301 (2015).

[2] V.V. Rondinella, Handb. Adv. Radioact. Waste Cond. Technol., 397-432 (2011).

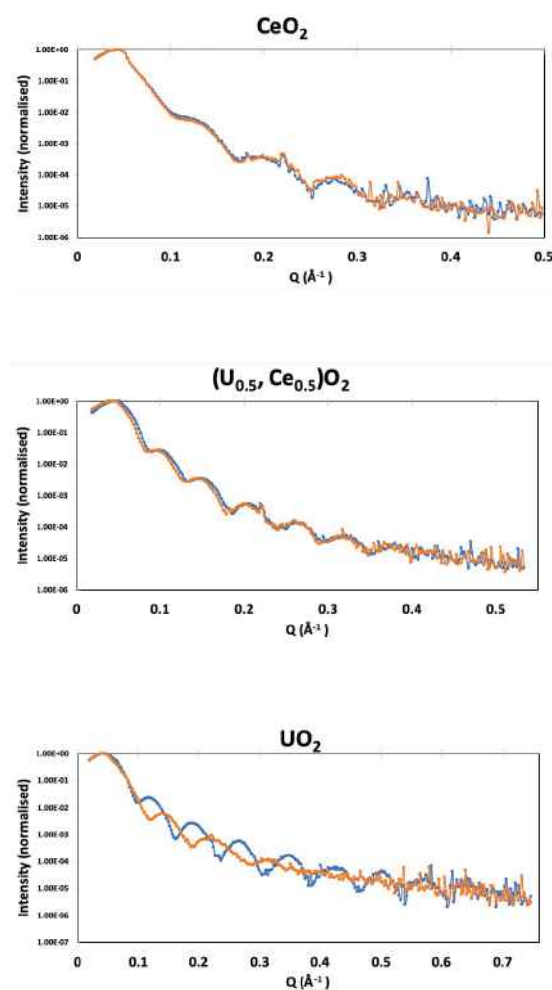


Fig. 6: XRR data of single crystal UO_2 , CeO_2 and $(\text{U}_{0.5}, \text{Ce}_{0.5})\text{O}_2$ thin films at 0s (blue) and 450 s (orange) of exposure to H_2O_2 . The fringe separation increase seen in the UO_2 data as a function of exposure time suggests corrosion. CeO_2 and $(\text{U}_{0.5}, \text{Ce}_{0.5})\text{O}_2$ remain unaffected by H_2O_2 . Similar results were observed for all other MOX film concentrations as well.

For more information contact:
S. Yadukrishnan, Department of
Engineering and Innovation,
The Open University, UK

ys982@open.ac.uk

Unravelling the magnetic proximity effect at interfaces

O. Inyang, B. Nicholson, M. Tokaç, R.M. Rowan-Robinson, C.J. Kinane, L. Bouchenoire, A.T. Hindmarch

In ultra-thin film multilayers, magnetism can be induced in nominally nonmagnetic metals, such as platinum, as a result of sharing an interface with an adjacent layer of ferromagnetic material. This proximity-induced magnetism (PIM) typically has a small magnetic moment, and decays over a length scale of roughly one nanometer. Such a small, localised, additional contribution to the total magnetisation is challenging to detect, making experimental investigation of PIM using conventional magnetometry difficult [1,2].

In this work, we have demonstrated how the magnitude of the PIM scales with the magnetisation of the ferromagnet in the interfacial region. In order to do this, we have used a combination of X-ray Resonant Magnetic Reflectivity (XRMR) and Polarized Neutron Reflectivity (PNR). PNR provides a quantitative

measure of the magnetisation in the ferromagnet, with depth resolution; since PIM is small both in amplitude and spatial extent, PNR is primarily sensitive to magnetism in the ferromagnetic layer. XRMR provides an element-specific probe of depth-resolved magnetism; in our case, it is sensitive only to any induced magnetism in platinum layers.

By using a designed trilayer sample of platinum layers sandwiching a CoFeTaB alloy, where the Curie temperature was tailored with local tantalum concentration, we were able to study the scaling between the PIM and interface magnetisation in the ferromagnet (Fig. 7). We used temperature to modulate the ferromagnet magnetisation. This allows us to probe this scaling over a wide range of ferromagnet magnetisation and employ the depth-resolution of PNR and XRMR to study both Pt/ferromagnet and

ferromagnet/Pt interfaces simultaneously [1].

These measurements show an unexpected deviation from the predicted linear scaling, requiring an initial magnetisation threshold in the ferromagnet before PIM begins to appear in the adjacent platinum layers. These results allow us to begin to explain the asymmetry found in PIM measurements by ourselves and others in a range of material systems [3,4].

- [1] O. Inyang *et al.*, Phys. Rev. B 100, 174418 (2019).
 [2] P. Bougiatioti *et al.*, Phys. Rev. Lett. 119, 227205 (2017).
 [3] R.M. Rowan-Robinson *et al.*, Sci. Rep. 7, 16835 (2017).
 [4] D.-O. Kim *et al.*, Sc. Rep. 6, 25391 (2016).

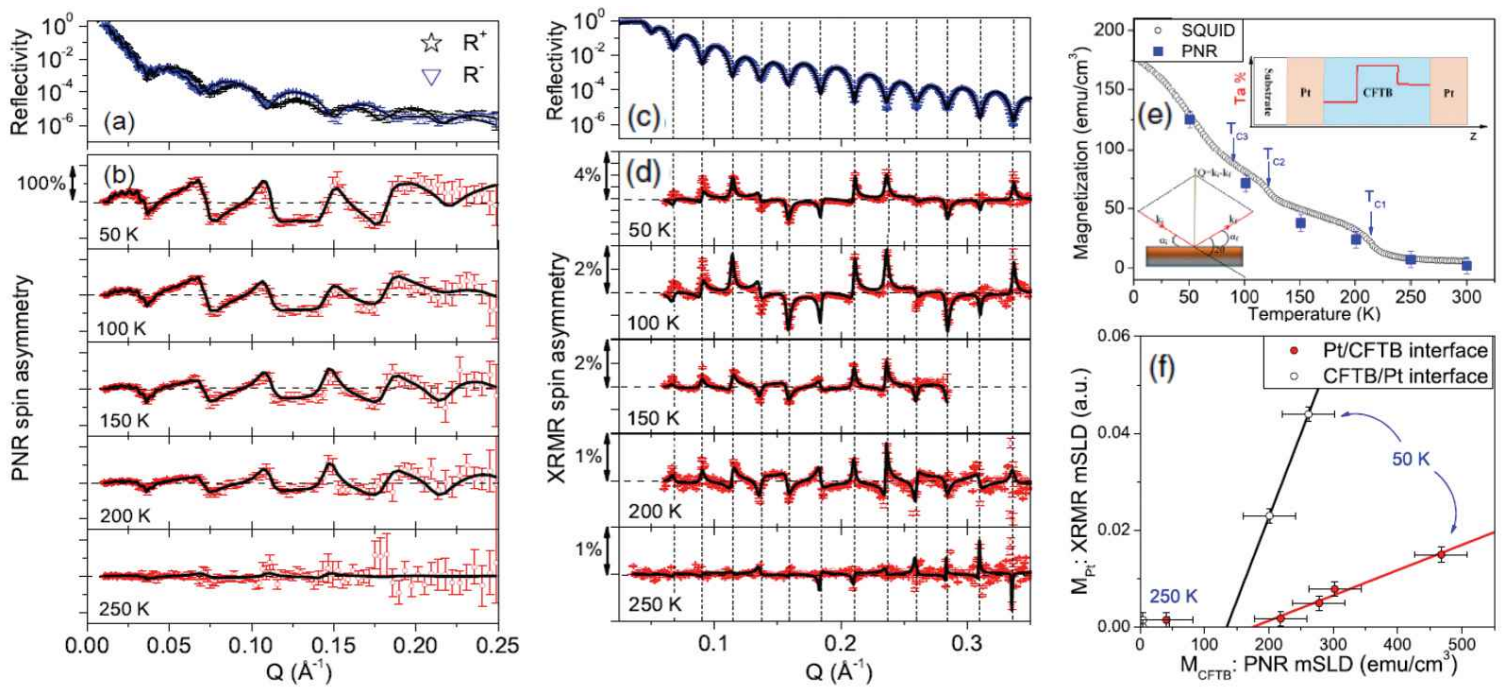


Fig. 7: Specular reflectivity (a, c) and spin-asymmetry (b, d) measured on a Pt/CoFeTaB/Pt trilayer sample using PNR (left panel) and XRMR (middle panel). The net magnetisation from PNR matches that measured by conventional magnetometry (e). The scaling between proximity induced magnetisation in Pt, from XRMR, and CoFeTaB interface magnetisation, from PNR, is shown in (f).

For more information contact:
 A.T. Hindmarch, Department of
 Physics, Durham University, UK.
 a.t.hindmarch@durham.ac.uk

Polymerisation rate dictates order and intrinsic strain generation in photo-cured dimethacrylate dental polymers

S. Sirovica, M.W.A. Skoda, M. Podgorski, P. Thompson, W.M. Palin, A.J. Smith, K. Dewan, O. Addison, R.A. Martin

Light activated resin-based composites are routinely used in dentistry as a filling material, largely replacing the use of mercury amalgams which are being phased out due to environmental and health concerns [1]. Dental composites combine an inorganic filler fraction with a resin phase (a blend of dimethacrylate monomers) and incorporate a photo-initiator species. Free radical polymerisation under light activation generates a highly cross-linked 3D polymer structure. This allows the clinician to set the material "on demand". However, the resin phase is highly sensitive to the curing regimen and accelerating polymerisation to reduce setting times impacts on the clinical efficacy and lifetime of the restoration [2]. The physico-mechanical properties of the composite are ultimately determined by the underlying polymer structure, but this is poorly understood. Our aim was, therefore, to elucidate the relationship between the polymerisation rate and the evolving polymer structure.

In-situ synchrotron x-ray scattering conducted at XMaS (ESRF) and I22 (DLS) was used to determine

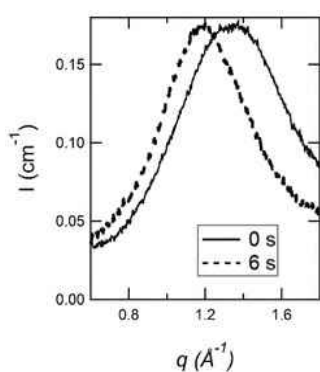
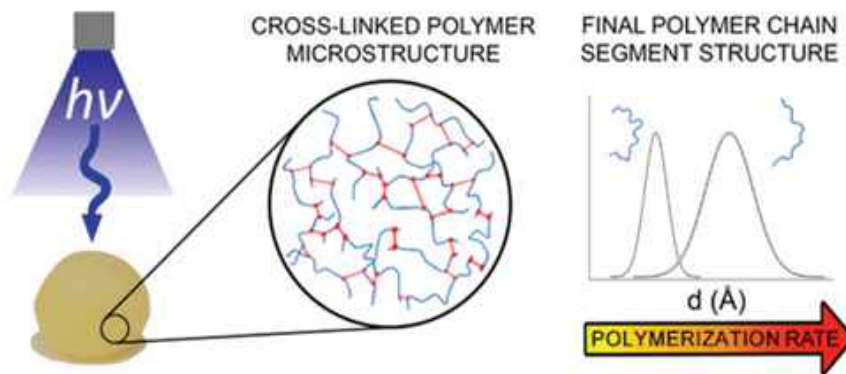


Fig. 8: X-ray scattering of a Bis-GMA/TEGDMA blend initiated with TPO before (solid line) and after 6s of irradiance (broken line). The shift of the peak to lower q and its narrowing are indicative of chain segment extension and an increase in the medium-range ($<10 \text{ \AA}$) relative structural order, respectively.



structural changes within the forming polymer network as a function of polymerisation rate. Briefly, clinically relevant monomers, Bis-GMA* and TEGDMA**, were combined in varying wt.% ratios incorporating either Lucirin TPO or Camphorquinone photo-initiator species (to provide relatively high and low radical yields, respectively). Monomer blends, in liquid load cells, were irradiated with a range of light intensities (to introduce systematically a range of polymerisation rates) whilst undertaking time resolved x-ray scattering and simultaneous Fourier Transform-Near Infrared (FT-NIR) measurements to monitor structural changes and reactive group conversion. Further experimental details can be found in the published article [3].

X-ray scattering measurements revealed that polymerisation induced polymer chain segment extension and modified medium-range structural order, predominantly within the reactive end groups of the monomers where C=C double bond conversion occurs (Fig. 8).

Accelerating polymerisation, through the use of high intensity light and Lucirin TPO photo-initiator, conferred greater chain extension in a shorter period of time but reduced the relative medium-range structural order per converted C=C double bond when compared with more

Fig. 9: (left) Cross-linked polymer structure of a light activated composite. (right) Scattering spectra for increasing chain extension and reduced structural order q and its narrowing are indicative of chain segment extension and an increase in the medium-range ($<10 \text{ \AA}$) relative structural order, respectively.

slowly polymerised systems (Fig. 9). At faster rates of polymerisation, the conformation of atoms at the reacting end group can become fixed into the polymer structure at the onset of auto-deceleration, storing residual strain.

Our results demonstrate that the curing protocol used by a dentist when photo-setting a resin composite filling can significantly influence the resultant polymer structure and residual strain stored within the material.

* Bis-GMA: bisphenol-A-glycidyl-methacrylate
** TEGDMA: triethyleneglycol-dimethacrylate

[1] Minamata Convention on Mercury. Geneva: United Nations Environment Programme (2013).

[2] R. Hickel *et al.*, *Am. J. Dent.* 18, 198 (2005).

[3] S. Sirovica *et al.*, *Macromolecules* 52, 5377 (2019).

For more information contact:
S. Sirovica, Faculty of Dentistry,
Oral and Craniofacial Science,
King's College London, London, UK.
slobodan.sirovica@kcl.ac.uk

Soft rectangular sub-3 nm tiling patterns by liquid crystalline self-assembly

A. Lehmann, A. Scholte, M. Prehm, F. Liu, X.B. Zeng, G. Ungar, C. Tschierske

Square and other rectangular nanoscale tiling patterns are of contemporary interest for soft lithography. Though soft square patterns on a ~ 40 nm length scale can be achieved with block copolymers, even smaller tiling patterns below 5 nm can be expected for liquid crystalline (LC) phases of small molecules. However, these usually form lamellar and hexagonal morphologies and thus the challenge is to specifically design LC phases forming square and rectangular structures, being compatible with industrial standards.

Two distinct types of liquid crystalline rectangular tiling patterns have been discovered, with the help of Grazing Incidence Small Angle X-ray Scattering (GISAXS) experiments carried out on surface aligned samples at BM28 in a series of T-shaped p-terphenyl based bolapolyphiles (Fig. 10 Scheme 1). By directed side chain engineering, sub-3 nm sized quadrangular honeycombs with rhombic ($c2mm$), square ($p4mm$, Fig. 11b-d) and rectangular ($p2mm$, Fig. 11e-g) shapes of the

cells were formed by spontaneous self-assembly [1]. The deformation of the square honeycombs to a rectangular one ($p2mm$) is attributed to an increasing anisotropy due to the growing contribution of straight and parallel *all-trans* segments at lowered temperature.

These rectangular honeycombs represent a new type of LC honeycomb, expanding the range of existing liquid crystalline quadrangular tilings. Quadrangular soft arrays of π -conjugated aromatics could also be of potential interest for the morphological design and patterning of self-assembled organic electronic materials.

[1] A. Lehmann *et al.*, *Adv. Funct. Mater.* 28, 1804162 (2018).

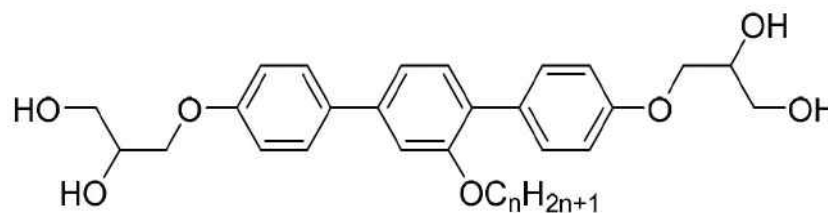


Fig. 10: Scheme 1. Chemical formulae of the T-shaped bola-polyphiles studied, $n=5-22$.

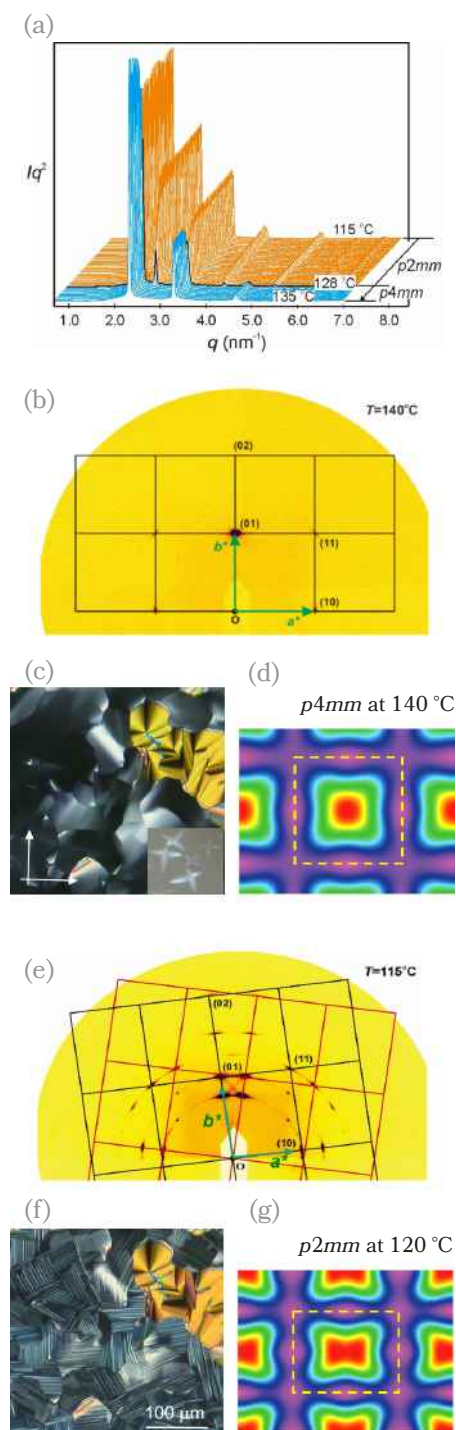


Fig. 11: Square and rectangular phases of compound $n=11$: (a) powder SAXS, (b) GISAXS pattern, (c) texture and (d) electron density map of the square phase. (e) GISAXS, (f) texture and (g) electron density map of the rectangular phase.

For more information contact:
X.B. Zeng, Department of Materials
Science and Engineering,
University of Sheffield, UK.

x.zeng@shef.ac.uk

Self-assembly of fluoride encapsulated POSS nanocrystals

E. Heeley, Y. El Aziz, C. Ellingford, A. Jetybayeva, C. Wan, E. Crabb, P. Taylor, A. Bassindale

Polyhedral oligomeric silsesquioxanes (POSS) are cage-like nanosized building blocks ($\text{RSiO}_{3/2}$)_n, where organic substituents are attached to the silicon-oxygen cage-like core having a wide variety of functionality and high thermal stabilities. We have synthesised a series of POSS compounds where a fluoride ion becomes encapsulated inside the cage in the presence of strongly electron withdrawing groups (EWG) perfluoroalkyl arms [$\text{CH}_2\text{CH}_2(\text{CF}_2)_n\text{CF}_3$] ($n = 3, 6, 8$ and 10). In our case, the counterion is tetrabutylammonium (TBA^+) or crown-ether⁺. Fig. 12 shows the structure of these POSS F-encapsulated molecules [1].

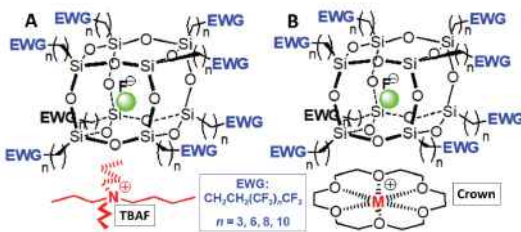


Fig. 12: Structure of POSS F-encapsulated molecules.

Due to the ionic nature of the F-encapsulated POSS molecules electrostatic interactions between charged groups and van der Waals forces of the EWG organic chains influence their nanocrystalline self-assembly in the solid state. Here, combined thermal and Small- and Wide-angle X-ray scattering (SAXS/WAXS), were used to investigate how the ordering and nanocrystalline packing morphology changes with temperature. Fig. 13 shows example 2D and 1D WAXS patterns of TBAF and crown molecules with perfluoroalkyl arms (denoted as TBAFC_n and crownC_n) at 30°C . The WAXS profiles are quite complex for the TBAF and crown molecules, showing many peaks in all cases and can assume that they all have triclinic unit cells determined from previous single crystal work [1]. From TGA* and DSC**, the melting temperatures (T_m) of these compounds were below

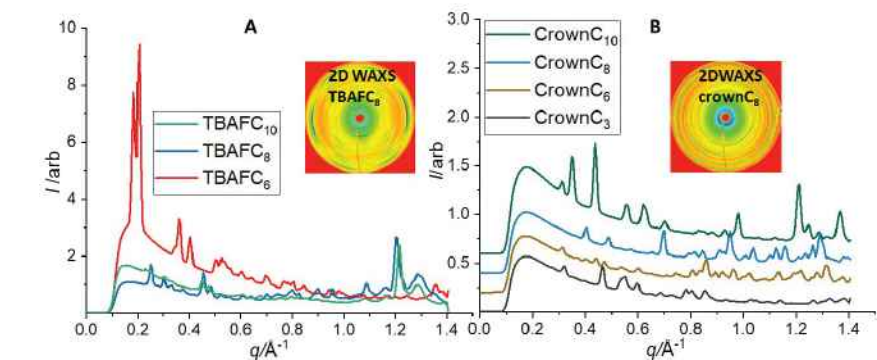


Fig. 13: 1D WAXS patterns of TBAF (A) and crown F-encapsulated POSS molecules (B). The insets show examples of 2D WAXS patterns.

100°C and showed thermal stability above T_m . The relatively low values of T_m are indicative of the nature of these molecules being potential ionic compounds.

Time resolved SAXS/WAXS was also used to follow the self-assembled nanocrystalline structure of these molecules with temperature. The major SAXS peaks for TBAFC_{10} and crownC_{10} gradually disappear on heating but return on cooling (Fig. 14). However, this is not the case for all the molecules, whereby the crystalline structure does not instantly re-order on cooling but takes several days to return [2].

Here, the self-assembled packing and ordering of the molecules were found to be of two types: those with shorter fluorinated alkyl chain arms (C_3 - C_6), packing are dominated by the ionic attraction between the cages so the arms form a disordered state that only reorder on standing; whereas those with longer fluorinated alkyl chain arms (C_8 - C_{10}) packing are dominated by the alignment of the arms into rod-like morphologies such that a fully ordered solid is formed from the melt [2].

*TGA: Thermogravimetric Analysis

**DSC: Differential Scanning Calorimetry

[1] Y. El Aziz, *et al.*, *Organometallics* 35, 4004 (2016).

[2] E. Heeley, *et al.*, *Cryst. Eng. Comm.* 21, 710 (2019).

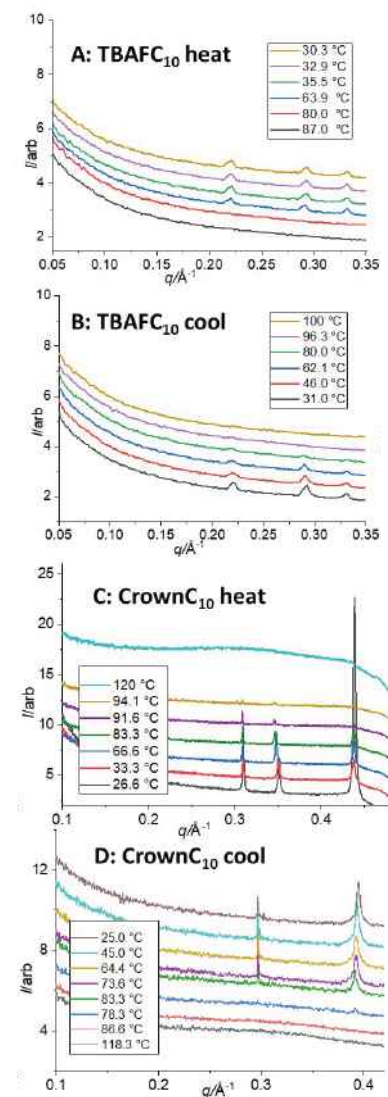


Fig. 14: Heat-cool 1D SAXS profiles of TBAFC_{10} (A, B) and crownC_{10} (C, D).

For more information contact:
E. Heeley, Faculty of STEM,
Open University, Milton Keynes, UK.
Ellen.Heeley@open.ac.uk

Identification and role of interstitial PdN_x structures in the selective oxidation of ammonia

E.K. Dann, E.K. Gibson, R.H. Blackmore, C.R.A. Catlow, P. Collier, A. Chutia, T. Eralp Erden, C. Hardacre, A. Kroner, M. Nachtegaal, A. Raj, S.M. Rogers, R. Taylor, P. Thompson, G.F. Tierney, C.D. Zeinalipour-Yazdi, A. Goguet, P.P. Wells

The harmful nature of NO_x emissions from automotive vehicles is well established and legislation on the quantities of permissible levels of NO_x within exhaust streams is becoming ever tighter. Current de-NO_x technologies utilise NH₃ to reduce NO_x to the environmentally benign N₂ (NH₃-SCR). The current drive to reduce NO_x emissions has led to de-NO_x technologies using greater amounts of NH₃. However, this has resulted in increased levels of unreacted toxic NH₃ in these exhaust streams. To remediate this issue, a selective NH₃ oxidation step (NH₃-SCO) downstream of the NH₃-SCR process has been introduced; the selectivity must be towards N₂ as over-oxidation will give rise to more unwanted NO_x. Supported Pd nanoparticles have proved highly active for NH₃-SCO, however, there is a strong temperature dependence on the selectivity of the process. This work describes *operando* spectroscopic studies during NH₃-SCO and makes direct correlations between the evolving structures of Pd nanoparticles (NPs) and the selectivity towards different products [1].

An initial combined time-resolved Pd K-edge X-ray Absorption Fine Structure (XAFS) and Diffuse Reflectance Infrared Fourier Transform Spectroscopy (DRIFTS) study was performed under NH₃-SCO conditions at the SuperXAS beamline (SLS). Assessing the gas composition as a function of temperature (Fig. 15), three distinct phases are observed: (i) an interstitial Pd species is formed during the low temperature regime (100°C ≤ T₁ ≤ 200°C), where the main product of NH₃ oxidation is N₂; (ii) Pd NPs with a bulk metallic structure and a surface oxide are formed in the mid-temperature regime (240°C < T₂ < 300°C), where an increasing

amount of NH₃ is oxidised to N₂O; (iii) bulk PdO NPs are formed at high temperature (T₃ > 300°C), which are linked to the production of NO.

Interstitial Pd hydrides and carbides are often determined through Pd K-edge X-ray Absorption Near Edge Spectroscopy (XANES) studies. In our work the only two interstitial structure types possible were Pd hydride and Pd nitride. Considering the process conditions, i.e. > 100°C, and the stability of Pd hydrides at these temperatures, we hypothesized that an interstitial nitride was the most likely structure – something that had not been previously reported. We needed an unambiguous method of determining the structure. To this aim, we used the XMaS beamline, where we performed *operando* NH₃ oxidation studies at the Pd L₃-edge. Pd hydride structures have a clear signature in the post-edge region of the Pd L₃ XANES, which was absent during our investigations, and allowed us to identify the PdN_x structure (Fig. 16).

This study has demonstrated the structure-function activity relationships for Pd NPs that arise during NH₃-SCO. Furthermore, it has identified a previously unreported PdN_x structure that forms during catalysis. This is a key finding, not only for NH₃ oxidation, but also in terms of identification of the PdN_x structure, which could have broader applicability to other areas in catalysis.

[1] E. Dann *et al.*, Nat. Catal. 2, 157 (2019).

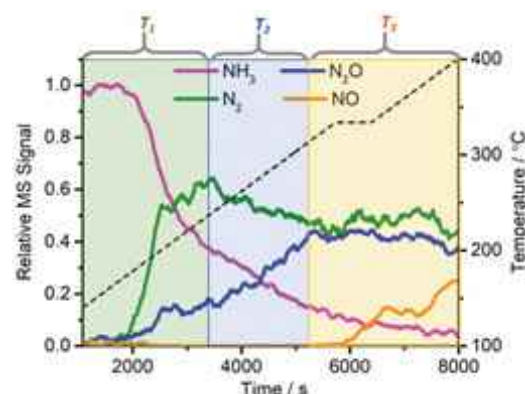


Fig. 15: Catalytic activity of 1.5 wt% Pd/γ-Al₂O₃ for NH₃ oxidation at increasing temperatures.

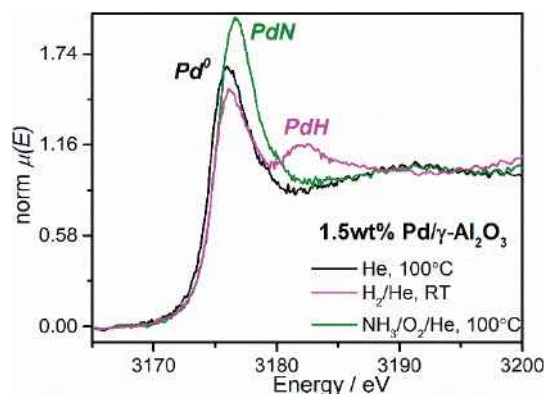


Fig. 16: *In-situ* Pd L₃-edge XANES of Pd/γ-Al₂O₃ in different gas environments.

For more information contact:
P.P. Wells, School of Chemistry,
University of Southampton, UK.
ppwells@soton.ac.uk

Electronic changes in LiFeSO₄F-PEDOT during Li-ion battery cycling

A. Blidberg, M. Valvo, M. Alfredsson, C. Tengstedt, T. Gustafsson, F. Björefors

With the growing demand for Li-ion batteries (LIBs) in electrical and hybrid vehicles, the cost and availability of the materials used to produce these batteries are becoming more important. To achieve affordable LIBs, the materials need to be abundant with low production costs. Iron-based materials can fulfil the requirements. In this study, the favorite-type structure (Fig. 17) of LiFeSO₄F has been studied using combined Fe and S K-edge X-ray Absorption Near Edge Spectroscopy (XANES) upon delithiation in LIBs [1].

The Fe-O bonds in polyatom anionic compounds are known to be more ionic in nature than in the basic oxides, caused by an inductive effect in the Fe-O-X linkage, resulting in the expectation that the capacity is solely linked to the Fe²⁺/Fe³⁺ redox couple [2]. However, studies on the iron silicates [3] have shown electron redistribution also in the polyatomic anion during battery cycling.

To improve the battery performance, the material was coated with p-doped PEDOT. The S K-edge absorption contributions of the PEDOT and LiFeSO₄F compounds were clearly separated (Fig. 17c) and, by performing a linear combination fit of the reference spectra, the composition was determined to be 76.4(5)% and 23.6(7)% of LiFeSO₄F and p-doped PEDOT, respectively. The PEDOT showed

good electrochemical stability in the voltage window studied here.

The reaction associated with Li half-cell charging:



is confirmed by the shift in the Fe K-edge absorption edge from lower (Fe²⁺) to higher (Fe³⁺) energies (Fig. 17b). The S K-edge of the LiFeSO₄F compound, show a shift of 0.9 eV towards higher energies during charging, confirming that there is also an electron redistribution around the polyanion. To confirm the change in electronic structure upon cycling, DFT (GGA+U) calculations on Li_xFeSO₄Cl (x=1-0) were performed, indicating that the charge on the S-atom increases as the material is delithiated, increasing the energy position of the unoccupied S s-orbitals (Fig. 18). The increased charge also results in shortening of the R(S-O) bond distances.

The increased iron-ligand electronic interaction upon delithiation is important in designing novel cathode materials with improved charge storage capability, making use of the simultaneous redox activity on both the transition metal and polyanion centre.

[1] A. Blidberg *et al.*, J. Power Sources 418, 84 (2019).

[2] M. Nakayana *et al.*, Chem. Mater. 16, 3399 (2004).

[3] M. Fehse *et al.*, J. Phys. Chem. C 123, 24396 (2019).

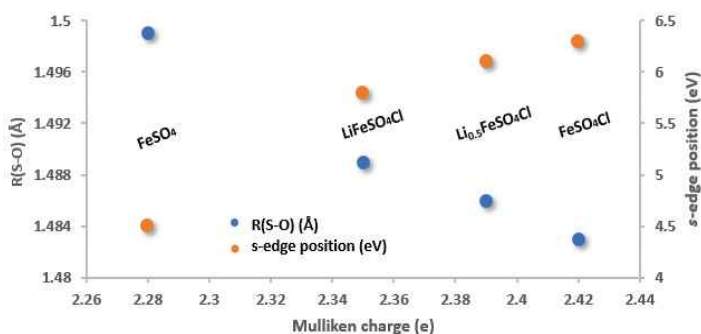


Fig. 18: DFT (GGA+U) calculations of S edge position and S-O bond distances as a function of the sulphur Mulliken charge.

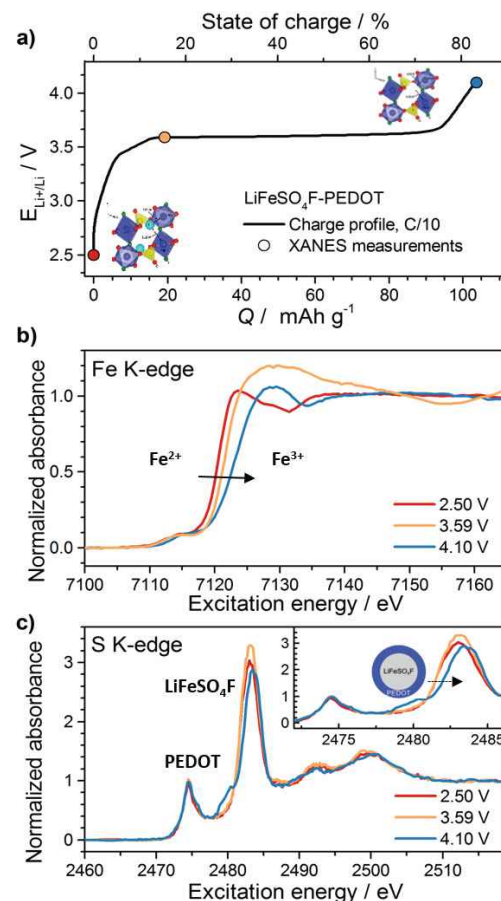


Fig. 17: (a) XANES evaluation of LiFeSO₄F-PEDOT composites cycled to different states of charge. The Fe K-edge spectra (b) and S K-edge spectra (c) showed no changes for PEDOT but indicated electronic changes on both the Fe and SO₄²⁻ anion.

For more information contact:
M. Valvo, Department of Chemistry,
Uppsala University, Sweden or
M. Alfredsson, School of Physical
Sciences, University of Kent, UK.

mario.valvo@kemi.uu.se
m.l.alfredsson@kent.ac.uk

APPLICATIONS FOR SYNCHROTRON BEAM TIME

Two proposal review rounds are held each year. **Deadlines for applications to make use of the national research facility (CRG) time are normally 1st April and 1st October** for the scheduling periods August to end of February and March to July, respectively.

Applications for beamtime must be submitted electronically via the ESRF web page: www.esrf.eu. Select "**Users & Science**", then choose "**Applying for beamtime**" from the drop-down list. On the right hand side, you can consult the instructions to submit your proposal and access the "**User Portal**". Enter your surname and password and select "**Proposals/Experiments**". Follow the instructions carefully — you must choose "**CRG Proposal**" and "**BM28 (XMaS - Mat.Sci.)**" at the appropriate stage in the process. If you experience any problems, please contact Laurence Bouchenoire (bouchenoire@esrf.fr). Technical specifications and instrumentation available are described on the XMaS web page (www.xmas.ac.uk). All sections of the form must be filled in. Particular attention should be given to the safety aspects with the name and characteristics of your samples completed carefully. Experiments requiring special safety precautions such as the use of electric fields, lasers, high pressure cells, dangerous substances, toxic substances and radioactive materials, must be stated clearly in the proposal. Moreover, any ancillary equipment supplied by the user must conform to the appropriate French regulations. Further information may be obtained from Martine Moroni, the ESRF Experimental Safety Officer for CRG beamlines (martine.moroni@esrf.fr, tel: +33 4 76 88 23 69). Please indicate your date preferences, including any dates that you would be unable to attend if invited for an experiment. This will help us to produce a schedule that is satisfactory for all.

When preparing your application, please consider that access to the national research facility is reserved for UK based researchers. Collaborations with EU and international colleagues are encouraged, but the proposal must be led by a UK based principal investigator. It must be made clear how any collaborative research supports the wider UK science base. Applications without a robust link to the UK will be rejected and should instead be submitted directly to the ESRF using their public access route.

Access to XMaS beamline is available for one third of its operational time to the ESRF's user community. Applications for beamtime within that quota should be made in the **ESRF's proposal rounds (application deadlines 1st March and 10th September)**. Applications for the same experiment may be made to both XMaS directly and to the ESRF. Obviously, proposals successfully awarded beamtime by the ESRF will not then be given additional time in the XMaS allocation.

An experimental report on completed experiments must be submitted electronically, following the ESRF model. The procedure for submitting experimental reports follows that for the submission of proposals. Please follow the instructions on the ESRF's web pages carefully. **Reports must be submitted within 6 months of the experiment.** Note that the abstract of a publication can also serve as the experimental report! Please also remember to fill in the XMaS end of run survey form on completion of your experiment, which is available on the website (<https://bit.ly/2FWfksW>).

Assessment of Applications

The Peer Review Panel considers the proposals, grades them according to scientific excellence, adjusts the requested beam time if required, and recommends proposals to be allocated beam time on the beamline. Experimental reports will also form part of the assessment criterion. Proposals which are allocated beamtime must meet ESRF safety and XMaS technical feasibility requirements. Following each meeting of the Peer Review Panel, proposers will be informed of the decisions taken and feedback provided.

APPLICATIONS FOR OFFLINE FACILITY TIME

Submit your application directly on the XMaS web site: www.xmas.ac.uk. Select "**XMaS Offline Facilities**" and then "**Application for Offline Facilities**". Follow the instructions carefully and do not forget to upload your 1-2 page proposal at the end of the application form. Please contact the local staff to discuss any potential experiments. Successful offline proposals will be run as in-house experiments. We will complete the safety form with the information supplied in your application form as well as arrange site passes and any accommodation that may be required. As for synchrotron beamtime, offline users normally stay in the ESRF guest house or off-site hotels.

The XMaS facility implements transparent policies and procedures to guarantee that access is based on scientific excellence only. In partnership with the ESRF Safety office, we will endeavor to ensure that the facility can accommodate any user, but this may require an individual needs assessment. If you have any questions about accessing the facility at any stage of the application or experimental processes, please do not hesitate to get in touch.

Living allowances

These are €70 per day per beamline user - the equivalent actually reimbursed in £. XMaS will support up to 3 users per synchrotron experiment and only 1 on the offline laboratories. For experiments which are user intensive, additional support may be available. The ESRF hostel still appears adequate to accommodate all our users, though CRG users will always have a lower priority than the ESRF's own users. Do remember to complete the "A-form" when requested to by the ESRF, as this is used for hostel bookings, site passes and to inform the safety group of attendees.

Beamline people

ONSITE TEAM

Didier Wermeille

didier.wermeille@esrf.fr

is the Beamline Responsible who, in partnership with the Directors, oversees the activities of the user communities as well as the programmes and developments that are performed on the beamline. He is also the beamline Safety Representative. His expertise spans between crystallography, high resolution diffraction, surface studies and electric field measurements.

Laurence Bouchenoire

bouchenoire@esrf.fr

is the Beamline Coordinator. She looks after beamline operations and can provide you with information about the beamline, application procedures, scheduling, etc. Laurence should normally be your first point of contact. Her expertise is in magnetic scattering including polarisation dependence.

Oier Bikondoa

oier.bikondoa@esrf.fr

is Beamline Scientist with expertise in soft matter materials, SAXS, GISAXS, GIWAXS, surface and reflectivity studies.

Paul Thompson

pthomps@esrf.fr

is the contact for instrument development, technical support, sample environments including electric field, liquid cells and catalysis. He is assisted by **John Kervin** jkervin@liv.ac.uk who is based at the University of Liverpool but provides further technical back-up and spends part of his time on-site at XMaS.

PROJECT DIRECTORS

Chris Lucas clucas@liv.ac.uk and **Tom Hase** t.p.a.hase@warwick.ac.uk continue to travel between the UK and France to oversee the operation of the beamline.

Malcolm Cooper

m.j.cooper@warwick.ac.uk

remains involved in the beamline operation as an Emeritus Professor at the University of Warwick.

Yvonne Gründer

yvonne.grunder@liverpool.ac.uk

joined the management team at Liverpool to provide additional support. She also oversees impact activities.

Natacha Borrel

n.borrel@warwick.ac.uk

and **Julie Clark**

Julie.Clark@liverpool.ac.uk

are the administrators on the project, based in the Department of Physics at Warwick and Liverpool, respectively. Natacha is the point of contact for user T&S claims and co-ordinates the annual XMaS Scientist Experience.

THE PROJECT MANAGEMENT COMMITTEE

The current membership of the committee is as follows:

P. Hatton (chair), University of Durham
A. Broomsgrove, EPSRC
S. Beaufoy, University of Warwick
M. Alfredsson, University of Kent
M. Cain, Electrosiences Ltd
A. Beale, University College London
K. Edler, University of Bath
B. Hickey, University of Leeds
S. Langridge, ISIS, Rutherford Appleton Laboratory
C. Nicklin, Diamond Light Source
W. Stirling, Institut Laue Langevin

In addition to the above, the directors, the chair of the Peer Review Panel, the CRG Liaison M. Hahn and the beamline team are in attendance at the meetings which happen twice a year.

THE PEER REVIEW PANEL

The current membership of the panel is as follows:

R. Johnson (chair), University of Oxford
W. Briscoe, University of Bristol
S. Corr, University of Glasgow
C. Detlefs, ESRF
J. Quintanilla, University of Kent
R. Walton, University of Warwick
J. Webster, ISIS, Rutherford Appleton Laboratory

In addition either Chris Lucas or Tom Hase attends their meetings in an advisory role.

PUBLISH PLEASE!!..... and keep us informed

One of the important XMaS KPIs is the number and quality of publications. We ask you to provide Natacha Borrel with the reference and DOI whenever a new paper is published. Alternatively, you can submit the reference of your new publication directly through a form on our web site (<https://tinyurl.com/yclguqdh>). Please also let us know about other impact generated as a result of XMaS work.

n.borrel@warwick.ac.uk

IMPORTANT!

It is important that we acknowledge the support from EPSRC in any publications. When beamline staff have made a significant contribution to your scientific investigation you may naturally want to include them as authors. Otherwise we ask that you add an acknowledgement of the form:

"XMaS is a UK national research facility supported by EPSRC. We are grateful to all the beamline staff for their support."

© Morel-ESRF





New Series Quadropod



6-Degrees of Freedom

Z Rz X Rx Y Ry

Minimum installation height
Increased power
Self-locking
Individually scalable:

- Precision
- Dimension
- Load carrying capacity
- Stability

Your Decision for Precision

www.xhuber.com



XMaS, the UK Materials Science Beamline
ESRF - The European Synchrotron,
71 avenue des Martyrs, CS 40220, 38043 Grenoble Cedex 9, France
Tel: +33 (0)4.76.88.25.80 / xmas@esrf.fr / [@XMaSBeam](https://twitter.com/XMaSBeam)

www.xmas.ac.uk